

# Quantification of cerebral circulation and shunt volume in a tentorial dural arteriovenous fistula using two-dimensional phase-contrast magnetic resonance imaging

Sung Won Youn<sup>1</sup>, Ho Kyun Kim<sup>1</sup>, Hui Joong Lee<sup>2</sup> and Jongmin Lee<sup>2</sup>

Acta Radiologica Short Reports  
2014, Vol. 3(5) 1–5  
© The Foundation Acta Radiologica  
2014  
Reprints and permissions:  
sagepub.co.uk/journalsPermissions.nav  
DOI: 10.1177/2047981614536559  
arr.sagepub.com



## Abstract

Venous hypertension is closely related to poor outcome of a dural arteriovenous fistula (DAVF). However, no direct measurements have been made of the shunt flow and impaired venous drainage that are suggestive of venous hypertension. We present a case of a 35-year-old man who presented with cerebral hemorrhage and underwent coil embolization for tentorial DAVF. Two-dimensional (2D) phase-contrast magnetic resonance imaging (MRI) was used to evaluate temporal changes in the flow volumes of the shunt and venous drainage between before and after embolization. The results demonstrated the feasibility of using 2D phase-contrast MRI to measure the shunt volume of a DAVF, which might be useful for assessing the improvement in cerebral circulation after embolization treatment.

## Keywords

Tentorium, arteriovenous fistula, therapeutic embolization, blood flow velocity, cerebral vein, cine MRI

Date received: 1 April 2014; accepted: 30 April 2014

## Introduction

Intracranial dural arteriovenous fistulas (DAVFs) account for 10–15% of all brain arteriovenous malformations, and consist of single or multiple fistulae whose nidus lies within dural leaflets (1). DAVFs with a tentorial dural location, comprising 4–8% of such fistulas, tend to show hemorrhage or progressive neurologic deficit (1–3). Venous hypertension due to impaired drainage is known to be the most-significant factor associated with these DAVFs (4).

Nevertheless, no direct and quantitative measurements have been made of either the shunt flow itself or the impaired venous drainage. Conventional magnetic resonance imaging (MRI) can detect tiny clusters of flow voids that are characteristic of an intracranial DAVF. Advanced MRI techniques involving the use of dynamic susceptibility contrast-enhancement (5), arterial spin labeling (6), and time-resolved 3D magnetic resonance angiography (MRA) (7) have enhanced the

sensitivity of non-invasive detection and the grading of intracranial DAVFs, but these techniques are still not able to quantify the shunt volume.

Two-dimensional (2D) phase-contrast MRI has proven useful for flow measurements in the various cervicocerebral vascular lesions (8–11), and hence is expected to be a promising method for directly measuring the shunt flow and its related impairments of venous drainage. This case report demonstrates the novel use of 2D phase-contrast MRI to measure the

<sup>1</sup>Department of Radiology, Catholic University of Daegu School of Medicine, Daegu, Republic of Korea

<sup>2</sup>Department of Radiology and Medical Engineering, Kyungpook National University School of Medicine, Daegu, Republic of Korea

## Corresponding author:

Sung Won Youn, Department of Radiology, Catholic University of Daegu School of Medicine, 3056-6 Daemyung-4 Dong, Nam-gu, Daegu 705-718, Republic of Korea.  
Email: ysw10adest@cu.ac.kr



shunt flow of a tentorial DAVF (TDAVF) and to assess the response of the cerebral circulation after treatment.

### Case report

A 35-year-old man presented with chronic headache and an abnormal sensation on the scalp. He had no history of injury, infection, or surgery of the central nervous system. Computed tomography (CT) showed symmetric calcification of the bilateral globus pallidus (Fig. 1a), and MRI revealed a small subcortical hemorrhage on the left temporal lobe (Fig. 1b). A large tubular and several tiny surrounding flow voids were detected on the midline tentorium (Fig. 1c). Digital subtraction angiography (DSA) revealed a TDAVF fed by the tentorial branches of the right and left meningohypophyseal trunk, which drained directly into the dilated venous pouch at the vein of Galen (Fig. 2). The fistulous connection was located at the midline tentorial edge and drained into the vein of Galen and straight sinus. Otherwise there was no other feeding supply from the external carotid and vertebral arteries. DSA indicated that cortical venous reflux was absent,

and the lesion was graded as type I in the Cognard classification (4).

Transvenous embolization was performed targeting the fistulous point by using detachable coils. A 6-Fr. guiding catheter (Envoy, Cordis Neurovascular, Miami Lakes, FL, USA) was positioned in the internal jugular vein, and a microcatheter (Excelsior-1018; Boston Scientific, Fremont, CA, USA) was navigated coaxially via a sigmoid–transverse–straight–sinuses approach. The guidewire was then carefully introduced and advanced to the fistulous point via the straight sinus, followed by the microcatheter. Embolization was performed using three detachable coils under guidance provided by angiographic road maps and fluoroscopic monitoring of the procedure using selective internal carotid angiography. Postembolization angiography confirmed that the fistula was occluded by sluggish contrast medium filling from feeding tentorial branches.

A 1.5-T MRI device (Signa Excite; GE Healthcare, Milwaukee, WI, USA) was used to acquire phase and magnitude data in a sequence of 2D fast cine phase-contrast images with retrospective peripheral gating as described previously (11). To assess the response to

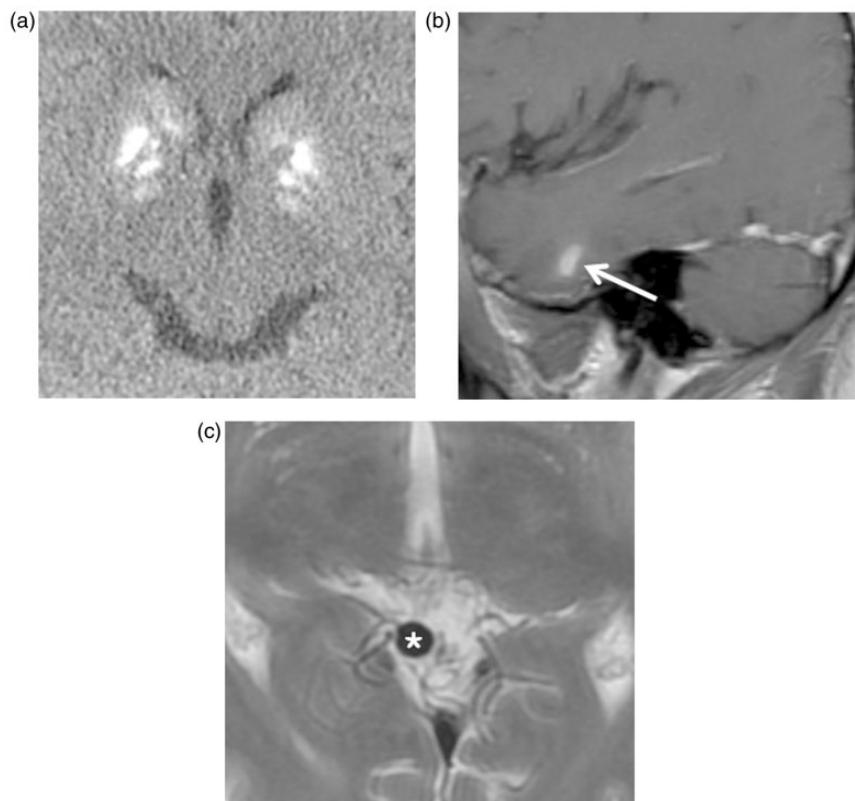


**Fig. 1.** Imaging of a 35-year-old man with headache. (a) CT shows symmetric calcifications of the bilateral globus pallidus. (b) Gadolinium-enhanced T1-weighted MRI reveals a small subcortical hemorrhage on the left temporal lobe (arrow). (c) T2W MRI shows a venous pouch (asterisk) and surrounding tiny engorged vessels on the midline tentorium.

treatment, MRI examinations were performed before, 1 day after, and 1 year after embolization. The MRI parameters were as follows: echo time, 4.4–7.1 ms; repetition time, 12.0–14.5 ms; views per segment, 4; flip angle, 28°; field of view, 28 mm<sup>2</sup>; matrix, 256 × 128; and slice

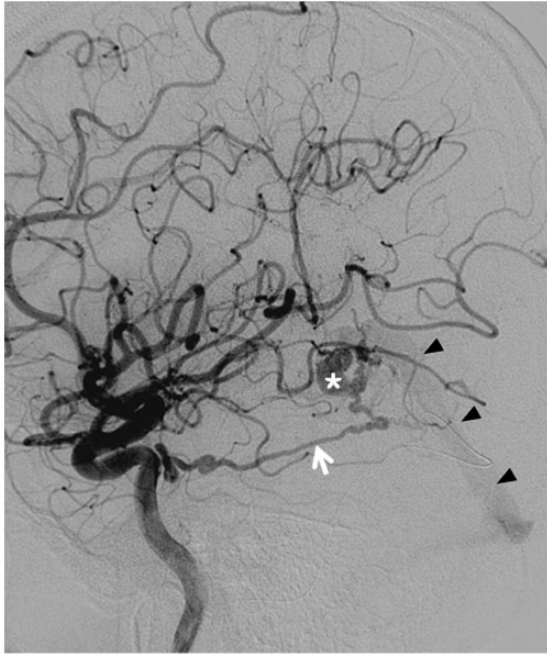


**Fig. 2.** Baseline digital subtraction angiography of the internal carotid artery. A tentorial dural arteriovenous fistula (TDAVF) was fed by the tentorial branch of the meningo-hypophyseal trunk (arrow), which drained directly into the dilated venous pouch (asterisk) at the vein of Galen. The fistulous connection drained into the straight sinus (arrowheads).

thickness, 5 mm. Velocity encoding was set at 80 cm/s. T2-weighted (T2W) midline sagittal images were used to select the anatomic levels for flow quantification. The acquisition planes were perpendicular to the direction of the flow at cervical levels 1 and 2, the midbasilar artery, and the coronal plane covering the tentorial feeders (Fig. 3).

Images were processed using software (ReportCARD, GE Healthcare, Milwaukee, WI, USA) to extract the region of interest and calculate the flow over 30 segments of the cardiac cycle. The flow volume (FV) of each vessel was calculated from the flow curve measured over one cardiac cycle.

The total FV of the tentorial feeding arteries was 235.8 mL/min (total FV of the right and left tentorial arteries; Table 1). This shunt volume was reduced to 120.6 and 15.4 mL/min at 1 day and 1 year after embolization, respectively. However, the FVs of the posterior cerebral and superior cerebellar arteries did not change

**Table 1.** FVs of tentorial feeding arteries and other arteries before, 1 day after, and 1 year after coil embolization of the tentorial dural arteriovenous fistula (TDAVF).

Location	FV, mL/min		
	Before	1 Day	1 Year
Right and left Tentorial A	235.8	120.6	15.4
Right and left PCA	328.6	375.1	246.0
Right and left SCA	113.0	131.6	69.3

PCA, posterior cerebral artery; SCA, superior cerebellar artery; Tentorial A, tentorial feeding artery.

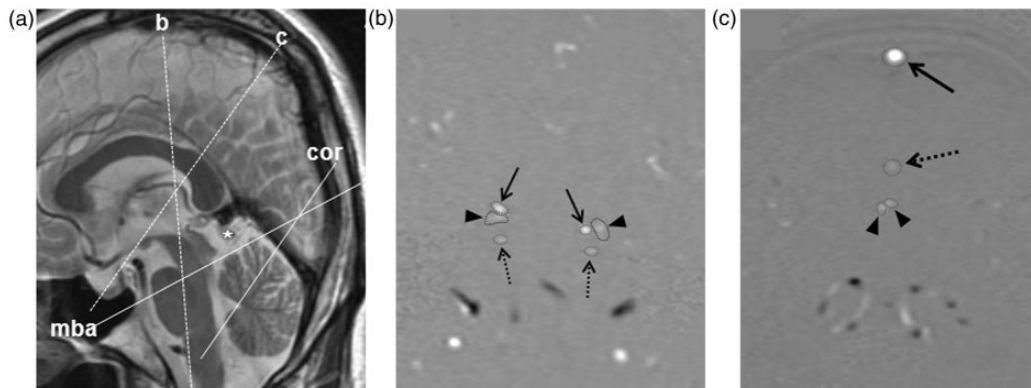


**Fig. 3.** Acquisition planes and region of interest. (a) On the T2W midline sagittal image, the acquisition planes were selected perpendicular to the direction of the flow at cervical levels 1 and 2 (image not shown), the midbasilar artery (mba), and the coronal plane (cor). The asterisk indicates the fistula. (b) The coronal plane covering the tentorial feeding arteries shows the posterior cerebral artery (solid arrows), superior cerebellar artery (dashed arrows), and tentorial artery (arrowheads). (c) The coronal plane covering the deep cerebral veins shows the superior and inferior sagittal sinus (solid arrows and dashed arrows) and the internal cerebral veins (arrowheads).

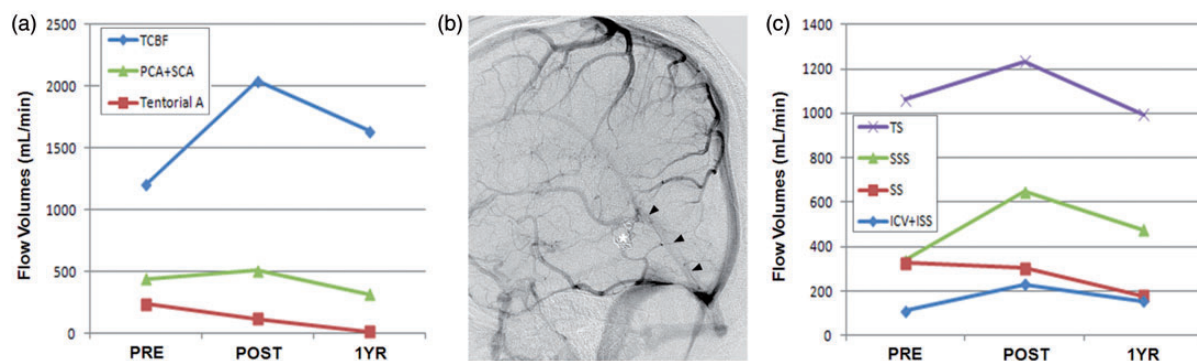


**Fig. 4.** Temporal changes in the FVs after coil embolization of the TDAVF. (a) FVs of the tentorial arteries (Tentorial A), posterior cerebral and superior cerebellar arteries (PCA + SCA), and total cerebral blood FV (TCBF), corresponding to the flows in the internal carotid arteries plus the basilar artery. Tentorial A or the shunt volume decreased progressively after embolization, PCA + SCA did not change significantly, and TCBF increased. (b) Lateral projection of the venous-phase angiogram immediately after coil embolization. The deep venous flows from the inferior sagittal sinus (ISS) and internal cerebral vein (ICV) drained into the straight sinus (SS, arrowheads) without hemodynamic disturbance from the TDAVF. The asterisk indicates the coiled TDAVF. (c) FVs in the venous drainage. SS or the direct drainage from the TDAVF decreased progressively after embolization, whereas ISS + ICV, SSS, and TS increased. SSS, FV of superior sagittal sinus; TS, FV of transverse sinus. PRE, POST, and 1YR are the time points before, 1 day after, and 1 year after embolization in (a) and (c).

**Table 2.** FVs of cerebral arteries and veins before, 1 day after, and 1 year after coil embolization of the TDAVF.

Location	FV, mL/min		
	Before	1 Day	1 Year
<i>Arteries at cervical levels 1 and 2 (C1–2)</i>			
Right and left ICA <sub>C1–2</sub>	950.9	1047.4	1022.5
Right and left VA <sub>C1–2</sub>	389.1	448.4	371.1
<i>Arteries at the midbasilar artery level (mba)</i>			
Right and left ICA <sub>mba</sub>	1151.5	1501.3	1236.8
BA	428.7	541.2	396.6
<i>Cerebral veins</i>			
ISS and ICV	138.7	228.3	154.4
SS	344.6	281.1	280.7
SSS	446.8	552.8	570.3
Right and left TS	1061.3	1234.7	993.2

BA, basilar artery; ICA, internal carotid artery; ICV, internal cerebral vein; ISS, inferior sagittal sinus; SS, straight sinus; SSS, superior sagittal sinus; TS, transverse sinus; VA, vertebral artery.

significantly after embolization, whereas the total FVs of the internal carotid and basilar or vertebral arteries were increased after embolization (Fig. 4a).

The baseline FV of the straight sinus, the direct draining vein of a TDAVF, was 327.5–344.6 mL/min, and reduced to 54.3–81.5% of the baseline value at 1 year after embolization (Table 2).

The FV of the inferior sagittal sinus plus internal cerebral veins, which are upstream deep venous

flows that are disturbed by a TDAVF, was 138.7 mL/min. The FV of the superior sagittal sinus, which are upstream superficial venous flows that are also disturbed by a TDAVF, was 411.1–446.8 mL/min. Both of these FVs were increased after embolization (Fig. 4b, c).

The patient outcome was uneventful during 1 year of clinical observation, and 1-year follow-up DSA showed stable occlusion of the TDAVF.

## Discussion

DSA can demonstrate the presence of cortical venous reflux or congestion in a TDAVF (4), but this technique is invasive and cannot be used to measure the volume of venous congestion quantitatively. Among the various advanced MRI techniques, time-resolved MRA can reveal retrograde cortical reflux, which is useful for the screening and monitoring of DAVFs (7). The arterial spin labeling technique shows perfusion changes related to DAVFs (6). However, there have been no direct quantitative measurements of the shunt flow itself, nor assessments of the improvement in the cerebral circulation after shunt obliteration. To our knowledge, this is the first report on the use of 2D phase-contrast MRI to measure the shunt volume.

The results demonstrated the feasibility of using 2D phase-contrast MRI to measure the FVs of the feeding arteries, direct draining vein, and disturbed cerebral veins of a TDAVF. The shunt volume accounted for 19.7% of the total FV of cerebral arteries, which was reduced to half of the baseline value at 1 day after

embolization and nearly to zero at 1 year after embolization. Progressive decreases in the FVs of the straight sinus (i.e. corresponding to direct draining vein of the TDAVF) were closely related to this decreased shunt volume. However, the FVs of other either deeply and superficially located cerebral veins, which had been disturbed by the TDAVF, were improved along with occlusion of the TDAVF. According to the Monro-Kellie doctrine (12), the venous engorgement in the TDAVF raises the intracranial pressure (ICP), which in turn decreases the cerebral perfusion pressure ( $CPP = \text{mean arterial pressure} - ICP$ ) and the cerebral blood flow ( $CBF = CPP / \text{resistance}$ ). Therefore, occlusion of the TDAVF removed the venous engorgement and subsequently normalized the ICP, CPP, and CBF.

2D phase-contrast MRI is safe and noninvasive since it does not require the injection of contrast medium. In addition, this study showed that the technique can be used to detect even minute changes that are not visualized by DSA. 2D phase-contrast MRI clearly demonstrated the impaired cerebral circulation due to venous hypertension, while DSA did not show cortical venous reflux in this patient. The patient had presented with subcortical hemorrhage and bilateral basal ganglia calcification, suggesting symptomatic and long-term venous hypertension. Moreover, although 2D phase-contrast MRI confirmed complete occlusion from the absence of residual flow at a 1-year observation, residual flow was still detected at half the pretreatment level at 1 day after embolization. In contrast, DSA appeared to show that the fistula was completely obliterated immediately after coil embolization.

Notwithstanding the limitation of being a single case report, this study suggests that 2D phase-contrast MRI is feasible for measuring the shunt volume and FVs of multiple vessels of a TDAVF, and to assess its therapeutic outcome by showing the changes in the cerebral circulation.

#### Conflict of interest

None declared.

#### Funding

This work was supported by the Basic Science Research Program through the National Research Foundation of Korea (NRF) funded by the Ministry of Education, Science and Technology (grant number NRF-2011-0014573).

#### References

1. Awad IA, Little JR, Akarawi WP, et al. Intracranial dural arteriovenous malformations: factors predisposing to an aggressive neurological course. *J Neurosurg* 1990; 72:839–850.
2. Tomak PR, Cloft HJ, Kaga A, et al. Evolution of the management of tentorial dural arteriovenous malformations. *Neurosurgery* 2003;52:750–760.
3. Zhou LF, Chen L, Song DL, et al. Tentorial dural arteriovenous fistulas. *Surg Neurol* 2007;67:472–481.
4. Cognard C, Gobin YP, Pierot L, et al. Cerebral dural arteriovenous fistulas: clinical and angiographic correlation with a revised classification of venous drainage. *Radiology* 1995;194:671–680.
5. Fujita A, Nakamura M, Tamaki N, et al. Haemodynamic assessment in patients with dural arteriovenous fistulae: dynamic susceptibility contrast-enhanced MRI. *Neuroradiology* 2002;44:806–811.
6. Noguchi K, Kuwayama N, Kubo M, et al. Flow-sensitive alternating inversion recovery (fair) imaging for retrograde cortical venous drainage related to intracranial dural arteriovenous fistula. *Neuroradiology* 2011;53: 153–158.
7. Farb RI, Agid R, Willinsky RA, et al. Cranial dural arteriovenous fistula: diagnosis and classification with time-resolved MR angiography at 3T. *Am J Neuroradiol* 2009;30:1546–1551.
8. Hendrikse J, Rutgers DR, Klijn CJ, et al. Effect of carotid endarterectomy on primary collateral blood flow in patients with severe carotid artery lesions. *Stroke* 2003; 34:1650–1654.
9. Neff KW, Horn P, Dinter D, et al. Extracranial-intracranial arterial bypass surgery improves total brain blood supply in selected symptomatic patients with unilateral internal carotid artery occlusion and insufficient collateralization. *Neuroradiology* 2004;46:730–737.
10. Dinter DJ, Buesing KA, Diehl SJ, et al. 2D cine phase-contrast MRI for volume flow evaluation of the brain-supplying circulation in moyamoya disease. *Br J Radiol* 2009;82:459–467.
11. Youn SW, Kim HK, Do YR, et al. Haemodynamic alterations in cerebral blood vessels after carotid artery revascularisation: quantitative analysis using 2D phase-contrast MRI. *Eur Radiol* 2013;23:2880–2890.
12. Ursino M, Giulioni M, Lodi CA. Relationships among cerebral perfusion pressure, autoregulation, and transcranial Doppler waveform: a modeling study. *J Neurosurg* 1998;89:255–266.